Turkish Journal of Electrical Engineering & Computer Sciences

http://journals.tubitak.gov.tr/elektrik/

Research Article

Turk J Elec Eng & Comp Sci
(2018) 26: 1505 – 1514

doi:10.3906/elk-1707-198

Higher order sliding mode controller for urea-SCR system

Palanikumar GURUSAMY[1], Uma GANDHI[1], Umapathy MANGALANATHAN[1,*], Arunshankar JAYABALAN[2]

[1]Department of Instrumentation and Control Engineering, National Institute of Technology, Tiruchirappalli, India
[2]Department of Instrumentation and Control Systems Engineering, PSG College of Technology, Coimbatore, India

Received: 15.07.2017 • **Accepted/Published Online:** 05.02.2018 • **Final Version:** 30.05.2018

Abstract: The urea-selective catalytic reduction (SCR) system is one of the effective after-treatment emission reduction methods for diesel engines that comply with the emission standards. This paper presents the development of a linear parameter-varying (LPV) model for the urea-SCR system from the identified linear models. To reduce the NO_X emissions from diesel engines, a LPV model-based supertwisting sliding mode controller with lemniscate sliding surface is designed. The closed-loop performance of the designed controller is evaluated through simulations for step change in input and disturbance in output. The controller performance is compared against the multimodel PI controller and LPV model-based supertwisting sliding mode controller with linear sliding surface. The use of smooth and robust lemniscate sliding surface provides faster response as compared to the other two controllers. The control algorithms are compared using the performance indices and the proposed control scheme has the least settling time and rise time.

Key words: Selective catalytic reduction, urea-SCR system, lemniscate sliding surface, supertwisting sliding mode controller, linear parameter-varying model

1. Introduction

In recent years, bounds on diesel engine emissions have been dramatically tightened by emission legislation. In order to comply with the stringent requirements, development of improved exhaust after-treatment systems is a challenge. The major emission pollutants from diesel engines are carbon monoxide (CO), unburned fuel, and NO_X. The oxidation of CO and unburned fuel can be carried out using a diesel oxidation catalyst. In an excess oxygen environment, typical diesel exhaust conversion efficiency of CO and unburned diesel fuel is satisfactory, but the efficiency of NO_X reduction is poor [1,2]. This in turn has motivated the development of promising technologies to achieve the required reduction rates for NOx such as exhaust gas recirculation, lean NOx traps, and selective catalytic reduction (SCR).

SCR technology is one of the most cost-effective and fuel-efficient technologies available to reduce diesel engine emissions. A major advantage of the SCR after-treatment system is the opportunity it provides to operate the engine fuel optimally, along with low particular matter emission and maximum reduction in NO_X. In the urea-SCR system, diesel exhaust fluid, an aqueous urea solution, is injected from an onboard supply tank, which decomposes to form ammonia through hydrolysis. The gas-phase ammonia is adsorbed onto the surface of the catalyst and then it reacts with gas-phase NO_X in the exhaust stream, resulting in harmless nitrogen (N_2) and water (H_2O) vapor [3].

*Correspondence: umapathy@nitt.edu

A 3-state lumped parameter model of the urea-SCR system for automotive applications using a 1-D model approach and a continuous stirred tank reactor approach have been developed [4]. The open-loop stability of the 3-state model and a sliding-mode controller for maximizing the NO_X reduction and minimizing slip ammonia have been studied [5]. A 4-state model by considering concentrations of NO and NO_2 separately has been proposed [6]. The adequacy of the 4-state model compared to higher order models in the control aspect and also a model-based state estimator and full state feedback nonlinear control for NO_X reduction have been demonstrated [7]. An adaptive model predictive control for NO_X reduction has been implemented [8]. The effectiveness of the linear parameter-varying (LPV) model for nonlinear model identification was demonstrated using a nonlinear model predictive controller based on the LPV model in [9] and it was concluded that the method is simple and can be used to model nonlinearity in gains and time constants.

In this paper, a LPV model for the urea-SCR system is developed considering output NO_X concentration as the scheduling parameter. The linear models are identified from the first principle model of the urea-SCR system with gas-phase concentration of NO_X, gas-phase concentration of ammonia, and surface coverage fraction of the catalyst (θ) as states. In the LPV model-based control scheme, a novel supertwisting sliding mode controller with lemniscate sliding surface is proposed. A LPV model-based supertwisting sliding mode controller (ST-SMC) with linear sliding surface and a multiple model-based control scheme with PI controller are implemented.

2. Description of urea-SCR system

The urea-SCR after-treatment system shown in Figure 1 consists of a catalytic reduction unit, a diesel exhaust fluid (DEF) tank, and its dosage valve. The DEF is a nontoxic homogeneous solution of 67.5% water and 32.5% automotive-grade urea. DEF decomposes into ammonia (NH_3) when sprayed into the hot exhaust gas stream. The inputs to the catalytic reduction unit are the NO_X from the diesel engine through the particulate filter and NH_3. The catalytic reduction unit reduces NO_X into nitrogen and water using NH_3 as a reductant. As NH_3 is considered a hazardous material, DEF has been specified as the standard precursor of ammonia for automotive application.

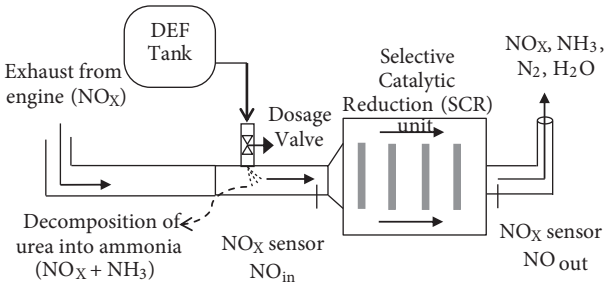

Figure 1. Schematic of the urea-SCR after-treatment system.

3. Modeling of urea-SCR system

Considering the gas-phase concentration of NO_X (C_{NO}), gas-phase concentration of NH_3 (C_{NH3}), and surface coverage fraction of the catalyst (θ_{NH3}) as three states, the combined dynamic equation of the urea-SCR after-treatment system is derived based on the molar balance using the continuously stirred tank reactor approach [4,5]. The nonlinear model of the urea-SCR system is given as:

$$\begin{aligned}
\frac{dC_{NO}}{dt} &= -C_{NO} f_{SC} r_{red} \theta_{NH3} + f_{SC} r_{oxi} \theta_{NH3} - \frac{F}{V_{cat}} C_{NO} + \frac{F}{V_{cat}} C_{NO}^{in} \\
\frac{d\theta_{NH3}}{dt} &= -\theta_{NH3} \left(r_{ads} C_{NH3} + r_{des} + r_{red} C_{NO} - r_{oxi} \right) + r_{ads} C_{NH3} \\
\frac{dC_{NH3}}{dt} &= -C_{NH3} f_{SC} r_{ads} \left(1 - \theta_{NH3} \right) + f_{SC} r_{des} \theta_{NH3} - \frac{F}{V_{cat}} C_{NH3} + \frac{F}{V_{cat}} C_{NH3}^{in}
\end{aligned} \tag{1}$$

Here, C_{NO}, θ_{NH3}, C_{NH3}, ϕ_{SC}, F, V_{cat}, C_{NO}^{in}, and C_{NH3}^{in} are the outlet concentration of NO_X, surface coverage fraction of the catalyst, outlet concentration of NH_3, total ammonia storage capacity of the catalyst, volumetric flow rate of the exhaust, volume of the catalyst, inlet concentration of NO_X, and inlet concentration of NH_3, respectively. r_{ads}, r_{des}, r_{oxi}, and r_{red} are reaction rates of the adsorption, desorption, oxidation, and reduction reaction, respectively, occurring in the catalytic unit. $\frac{F}{V_{cat}}$ is defined as the space velocity or normalized flow of the exhaust from the engine.

The first and second order linear models of the urea-SCR system given in Eq. (2) and (3) are identified from the open-loop step response of the system in Eq. (1). The step change is given in input (C_{NH3}^{in}) from 0 PPM to 100 PPM in steps of 25 PPM as shown in Figure 2. The gain (K) and time constants (τ, τ_1, and τ_2) for the models of four regions are given in Tables 1 and 2.

$$G_F(s) = \frac{y_F(s)}{r(s)} = \frac{K}{\tau s + 1} \tag{2}$$

$$G_S(s) = \frac{y_S(s)}{r(s)} = \frac{K}{(\tau_1 s + 1)(\tau_2 s + 1)} \tag{3}$$

Here, τ, τ_1, and τ_2 are the time constants and K is the process gain

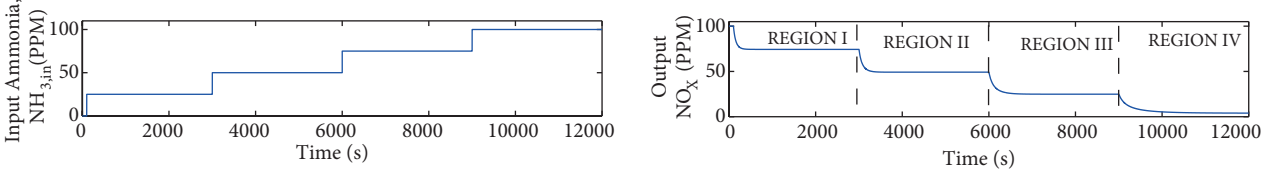

Figure 2. Open-loop response of the urea-SCR system.

Table 1. First order linear model parameters of the urea-SCR system.

Operating region/transfer function	Process gain (K)	Time constant (τ_1)	Fit percentage (%)
Region 1/G_{F1}(s)	2.9718	57.97	87.94
Region 2/G_{F2}(s)	0.9838	82.97	96.07
Region 3/G_{F3}(s)	0.3327	134.12	94.83
Region 4/G_{F4}(s)	0.0413	303.01	89.23

The linear models obtained above for each operating region are validated with the nonlinear model in Eq. (1) by applying a similar kind of step input. The fit percentage calculated from the normalized root mean square error method is found to be higher for second order models.

Table 2. Second order linear model parameters of the urea-SCR system.

Operating region/transfer function	Process gain (K)	Time constant 1 (τ_1)	Time constant 2 (τ_2)	Fit percentage (%)
Region 1/$G_{S1}(s)$	2.9748	47.85	9.89	96.60
Region 2/$G_{S2}(s)$	0.9831	106.93	55.21	98.08
Region 3/$G_{S3}(s)$	0.3314	183.29	67.71	98.83
Region 4/$G_{S4}(s)$	0.0392	521.18	124.52	99.03

4. LPV model for urea-SCR system

The LPV model has proven to give a good approximation of many nonlinear industrial processes. The nonlinear model can be replaced with the less complex LPV model, which is an interpolation of linear models. The main advantage of the LPV model is that it can model both static and dynamic nonlinearity. The LPV models are proven to be efficient for processes with larger transients where quicker changes in operating conditions occur. Due to these factors, in this work the LPV model of the urea-SCR system is developed using the first and second order linear models in Eqs. (2) and (3).

The general form of the LPV model obtained from interpolation of the linear models using triangular weights [10] is given by the following:

$$G_{LPV}(s) = \left\{ \begin{array}{ll} G_1(s); & C_{NO}^{in}(t) \geq r_1 \\ w_1\left(C_{NO}^{in}(t)\right) G_1(s) + w_2\left(C_{NO}^{in}(t)\right) G_2(s); & r_1 > C_{NO}^{in}(t) \geq r_2 \\ w_2\left(C_{NO}^{in}(t)\right) G_2(s) + w_3\left(C_{NO}^{in}(t)\right) G_3(s); & r_2 > C_{NO}^{in}(t) \geq r_3 \\ w_3\left(C_{NO}^{in}(t)\right) G_3(s) + w_4\left(C_{NO}^{in}(t)\right) G_4(s); & r_3 > C_{NO}^{in}(t) \geq r_4 \\ G_4(s); & r_4 \geq C_{NO}^{in}(t) \end{array} \right\} \tag{4}$$

Here, $G_1(s), G_2(s), G_3(s)$, and $G_4(s)$ are the transfer functions of linear regions I, II, III, and IV, respectively. The output of the LPV model obtained using first order linear models $y_F(t)$ and second order linear models $y_S(t)$ are defined as [9,10]:

$$y_F(t) = w_1(C_{NO}^{in}) y_{F1}(t) + w_2(C_{NO}^{in}) y_{F2}(t) + w_3(C_{NO}^{in}) y_{F3}(t) + w_4(C_{NO}^{in}) y_{F4}(t) \tag{5}$$

$$y_S(t) = w_1(C_{NO}^{in}) y_{S1}(t) + w_2(C_{NO}^{in}) y_{S2}(t) + w_3(C_{NO}^{in}) y_{S3}(t) + w_4(C_{NO}^{in}) y_{S4}(t) \tag{6}$$

Here, $y_{F1}(t), y_{F2}(t), y_{F3}(t)$, and $y_{F4}(t)$ are the outputs of first order linear models corresponding to regions I, II, III, and IV and $y_{S1}(t), y_{S2}(t), y_{S3}(t)$, and $y_{S4}(t)$ are the outputs of second order linear models corresponding to regions I, II, III, and IV. $\mathrm{w}_1\left(C_{NO}^{in}(t)\right)$, $\mathrm{w}_2\left(C_{NO}^{in}(t)\right)$, $\mathrm{w}_3\left(C_{NO}^{in}(t)\right)$, and $\mathrm{w}_4\left(C_{NO}^{in}(t)\right)$ are weighting functions. The weighting functions are formulated based on the variation in the concentration of NO_X $\left(C_{NO}^{in}(t)\right)$, which is considered as the scheduling variable. The weighting functions are determined using triangular weights and are given as follows:

$$\begin{array}{l} w_1\left(C_{NO}^{in}\right) = \frac{\alpha_2 - C_{NO}^{in}(t)}{\alpha_2 - \alpha_1}, w_2\left(C_{NO}^{in}\right) = \frac{\alpha_3 - C_{NO}^{in}(t)}{\alpha_3 - \alpha_2}, \\ w_3\left(C_{NO}^{in}\right) = \frac{\alpha_4 - C_{NO}^{in}(t)}{\alpha_4 - \alpha_3}, w_4\left(C_{NO}^{in}\right) = \frac{C_{NO}^{in}(t) - \alpha_3}{\alpha_3 - \alpha_4}. \end{array} \tag{7}$$

Here, α_1, α_2, α_3, and α_4 are the nominal values of the scheduling parameter (C_{NO}^{in}) for each operating region and are obtained from the open-loop response shown in Figure 2. The LPV model output represented with a transfer function corresponding to each operating region can be written as follows:

$$y_F(t) = w_1(C_{NO}^{in})G_{F1}r_1 + w_2(C_{NO}^{in})G_{F2}r_2 + w_3(C_{NO}^{in})G_{F3}r_3 + w_4(C_{NO}^{in})G_{F4}r_4 \tag{8}$$

$$y_S(t) = w_1(C_{NO}^{in})G_{S1}r_1 + w_2(C_{NO}^{in})G_{S2}r_2 + w_3(C_{NO}^{in})G_{S3}r_3 + w_4(C_{NO}^{in})G_{S4}r_4 \tag{9}$$

Here, $G_{F1}(s)$,$G_{F2}(s)$,$G_{F3}(s)$, and $G_{F4}(s)$ are first order linear transfer functions; $G_{S1}(s)$, $G_{S2}(s)$,$G_{S3}(s)$, and $G_{S4}(s)$ are second order linear transfer functions; and $r_1(s)$, $r_2(s)$, $r_3(s)$, and $r_4(s)$ are respective step inputs to the models.

The LPV model obtained using the first order and second order linear models is validated with the nonlinear model of Eq. (1) and the results are shown in Figure 3. From these results it is observed that the LPV model obtained using second order linear models is in very close agreement with the response of the nonlinear model and hence this model is considered for designing a controller.

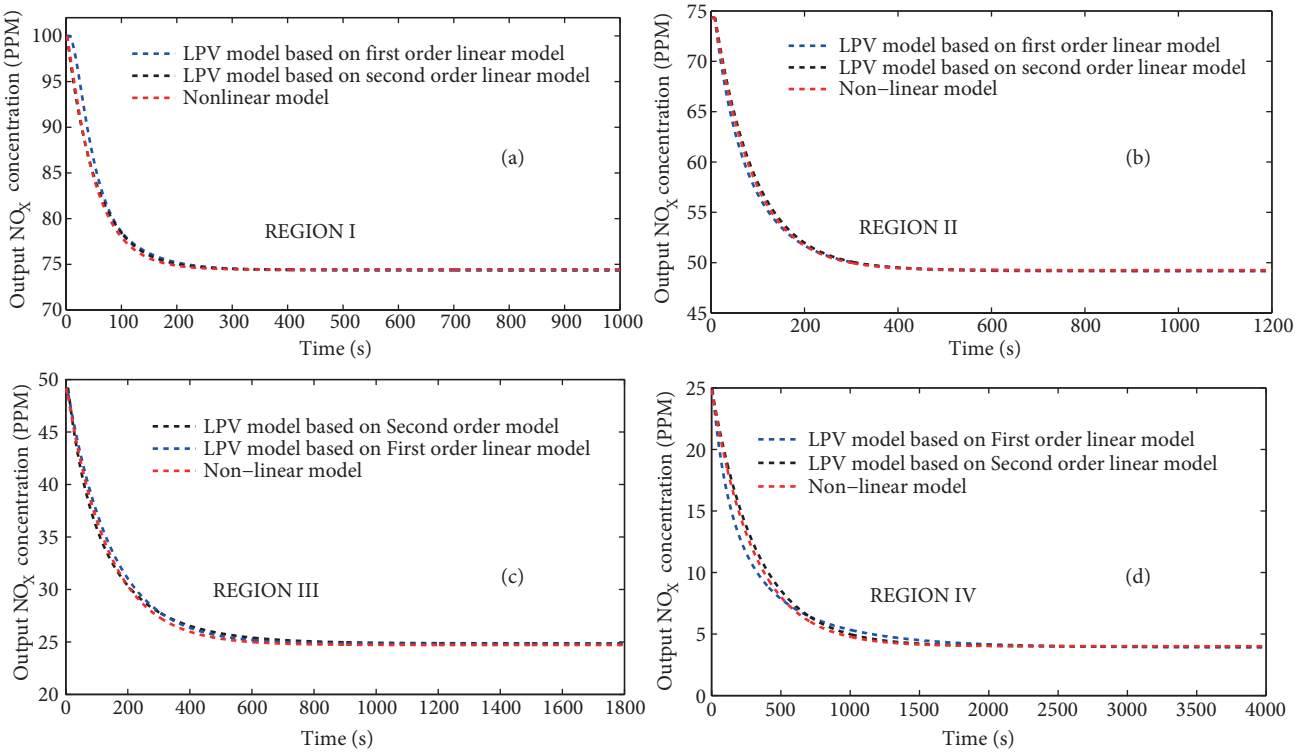

Figure 3. Validation of LPV models with open-loop response of the nonlinear urea-SCR model: (a) region I, (b) region II, (c) region III, (d) region IV.

5. Controller design

In this section, the ST-SMC with lemniscate sliding surface for the control of NO_X concentration at the outlet of the urea-SCR system is designed by using the LPV model derived in Section 4. The control signal for each region is generated using the model corresponding to that region and a single control signal $u(t)$ for the LPV

model in Eq. (4) is generated using the weights computed in Eq. (7). The control signal $u(t)$ is:

$$u(t) = w_1(C_{NO}^{in})u_1(t) + w_2(C_{NO}^{in})u_2(t) + w_3(C_{NO}^{in})u_3(t) + w_4(C_{NO}^{in})u_4(t) \tag{10}$$

Here, $u_1(t)$, $u_2(t)$, $u_3(t)$, and $u_4(t)$ are the controller outputs of the linear region models.

The control (u) is designed in two parts, namely equivalent control u_{eq} (continuous control) and supertwisting sliding mode control u_{STC} (discontinuous control). The control u is defined as follows [11,12]:

$$u_{i,i=1,2,3,4} = u_{eq} + u_{STC} \tag{11}$$

As a first step to derive a continuous control u_{eq}, a lemniscate-based sliding surface [13] is designed for each linear model. The sliding surface is defined as follows:

$$S = \left(\frac{e^2}{a^2} + \frac{\dot{e}^2}{b^2}\right)^2 - \left(\frac{e^2}{a^2} + \frac{\dot{e}^2}{b^2}\right) \tag{12}$$

Here, e is the error between desired (r) and measured (y) NO_X concentration, and a and b are scaling factors for the x-axis and y-axis, respectively. The desired NO_X concentration (r) is constant and hence $\ddot{e} = \ddot{y}$. The equivalent control (u_{eq}) is derived by equating $\dot{S} = 0$:

$$\dot{S} = 2\dot{e}\left\{\frac{2e^3}{a^4} + \frac{2\dot{e}^2\ddot{e}}{b^4} + \frac{2}{a^2}\left(e\dot{e}^2 + e^2\ddot{e}\right) - \frac{e}{a^2} + \frac{\ddot{e}}{b^2}\right\} = 0 \tag{13}$$

$$\ddot{e} = \frac{\left(\frac{e}{a^2} - \frac{2\dot{e}e^2}{a^2} - \frac{2e^3}{a^4}\right)}{\left(\frac{2\dot{e}^2}{b^4} + \frac{2e^2}{a^2} + \frac{1}{b^2}\right)} \tag{14}$$

Furthermore, by substituting $\ddot{e}$ in Eq. (3) and solving for u:

$$\ddot{e} = \ddot{y} = \left[Ku - (\tau_1 + \tau_2)\,\dot{y} - y\right]\frac{1}{\tau_1\tau_2} \tag{15}$$

$$u_{eq} = -\frac{1}{K}e\,(\tau_1\tau_2)\left[\frac{b^2\left(\frac{2e^2}{a^2} + \frac{2\dot{e}^2}{b^2} - 1\right)}{a^2\left(\frac{2e^2}{a^2} + \frac{2\dot{e}^2}{b^2} + 1\right)}\right] + \frac{1}{K}\left[\dot{e}\,(\tau_1 + \tau_2) - r\right] \tag{16}$$

The control u_{STC} is defined as follows [14,15]:

$$u_{STC} = \lambda_1 sgn(S)\,|S|^{\frac{1}{2}} + \lambda_2 \int sgn(S)dt \tag{17}$$

Here, λ_1 and λ_2 are tunable gains.

The sliding surfaces designed for each operating region are shown in Figure 4. The tunable gains in u_{STC} given in Eq. (17) for the operating regions are as follows: for region I, $\lambda_1 = 1$, $\lambda_2 = 0.1$; for region II, $\lambda_1 = 1.35$, $\lambda_2 = 0.25$; for region III, $\lambda_1 = 1.8$, $\lambda_2 = 0.7$; and for region IV, $\lambda_1 = 2.4$, $\lambda_2 = 1.6$. As there are no methods or rules of thumb available for selection of λ_1 and λ_2, they have been selected based on prior knowledge. Considering the variation in process gain and time constant, initial values of λ_1 and λ_2 were selected and tuned by trial and error for optimal performance.

6. Results and discussion

Performance of the controller designed in Section 5 is evaluated through simulation. In the performance evaluation, region I, having a setpoint of 85 PPM NO_X concentration, is considered. A step change of +5% at 300 s and –5% at 900 s is applied at the setpoint of NO_X concentration. The response of the plant and control signal is shown in Figure 5 and it can be observed that the controller tracks the change in NO_X concentration to the desired levels of 89.25 PPM and 80.75 PPM, respectively. The rise time and settling time are 22 s and 54 s, respectively. A disturbance of 10 PPM NO_X concentration is introduced at 300 s and the response is shown in Figure 6. It can be observed that the controller brings the output back to the desired value within 51 s. This performance evaluation is carried out in other regions in a similar way and the results are shown in Figures 7 and 8. The rise time and settling time measured for each region are given in Table 3. Further, a step change of 5% in NO_X concentration is applied at 600 s and the control signal is switched OFF at this instant to demonstrate the effectiveness of the controller. It can be seen from Figure 9 that the output NO_X concentration is found to increase and then the control signal is switched ON when the rate of change of NO_X concentration is maximum. The controller is able to bring the NO_X concentration to the desired value within 48 s, as shown in Figure 9.

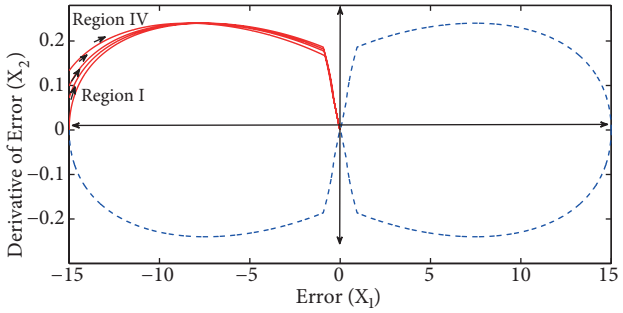

Figure 4. Lemniscate-shaped trajectory of the sliding surface and phase portrait of the system in all regions.

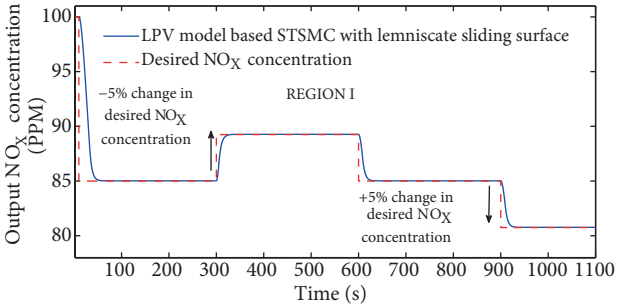

Figure 5. Setpoint tracking of the proposed LPV model-based ST-SMC with lemniscate surface, region I.

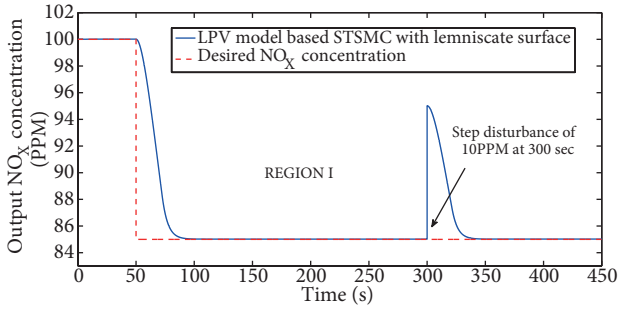

Figure 6. Disturbance rejection of the proposed LPV model-based ST-SMC with lemniscate surface, region I.

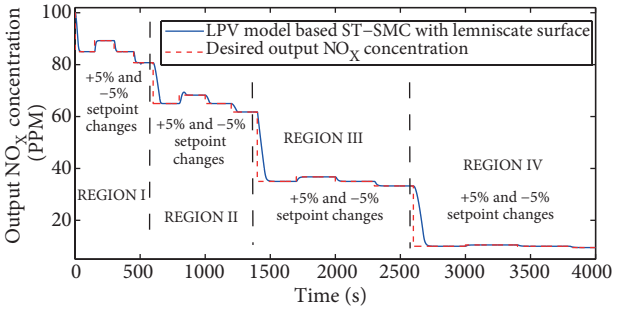

Figure 7. Setpoint tracking of the proposed LPV model-based ST-SMC with lemniscate surface in all regions.

To compare the performance of the proposed LPV model-based ST-SMC with lemniscate sliding surface, a multimodel PI controller using direct synthesis method [16] and a LPV model-based ST-SMC with linear sliding surface are designed. For the PI controller, the proportional gain (K_P) and integral time (τ_i) are designed for all four regions as $K_P = 1/K$ and $\tau_i = \tau_1$, where K and τ_1 are the process gain and time constant of second order linear models corresponding to that region. Based on the region in which the output NOx

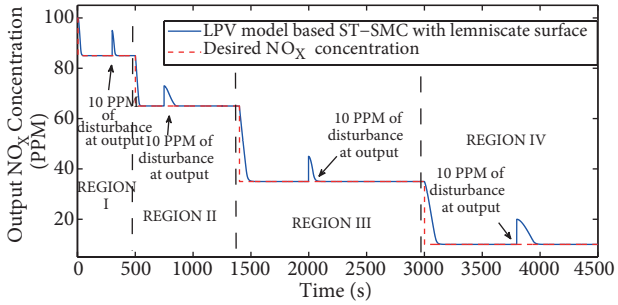

Figure 8. Disturbance rejection of the proposed LPV model-based ST-SMC with lemniscate surface in all regions.

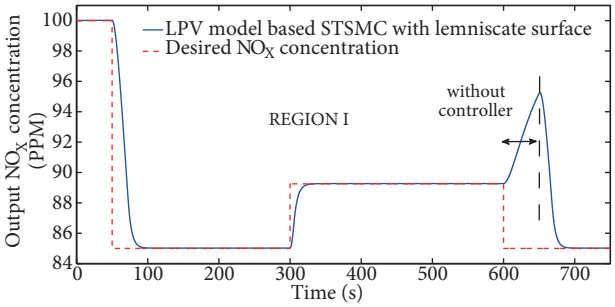

Figure 9. Performance of the system with and without the proposed LPV model-based ST-SMC with lemniscate surface, region 1.

Table 3. Performance indices of the proposed LPV model-based ST-SMC with lemniscate surface in all regions.

	Proposed LPV ST-SMC with lemniscate surface		LPV ST-SMC with linear surface		Multimodel PI controller	
	Settling time (s)	Rise time (s)	Settling time (s)	Rise time (s)	Settling time (s)	Rise time (s)
Region I	54	22	224	67	306	97
Region II	128	27	327	70	575	128
Region III	197	58	442	103	712	193
Region IV	261	72	549	131	964	262

concentration lies, the controller switches parameters K_P and τ_i. The urea-SCR system with multimodel PI controller is evaluated by introducing similar setpoint change and disturbance in output as applied to evaluate the proposed controller and the responses are shown in Figures 10 and 11. The settling time and rise time in region I are 306 s and 121 s, respectively.

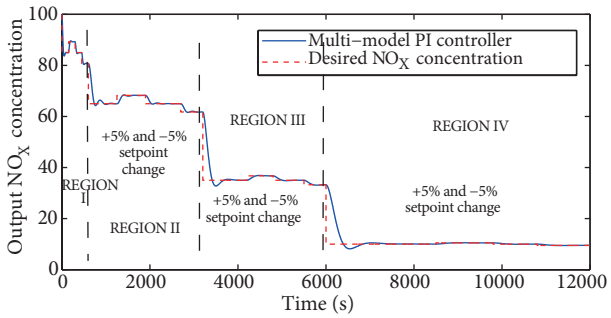

Figure 10. Setpoint tracking of the multimodel PI controller in all regions.

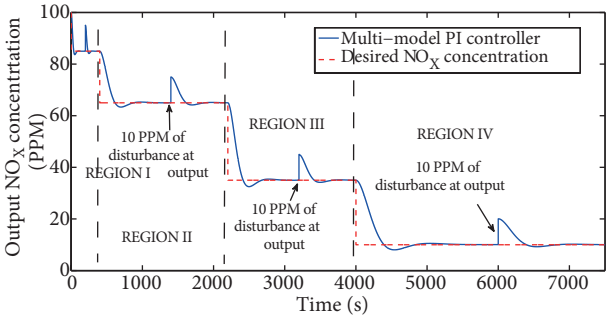

Figure 11. Disturbance rejection of the multimodel PI controller in all regions.

In the LPV model-based ST-SMC with linear sliding surface, the sliding surface is designed for all four regions separately as $S = (c \times e) + \dot{e}$, where c is tunable gain. The control signal u defined in Eq. (10) is computed and applied to the system. Here, the equivalent control (u_{eq}) in Eq. (11) for each linear region is given by $u_{eq} = \frac{1}{K}\left[(\tau_1 + \tau_2 - c\tau_1\tau_2)\,\dot{e} + e + r\right]$, where K, τ_1, and τ_2 are process gain time constants corresponding

to each region and the discontinuous control u_{STC} is the same as the one defined in Eq. (17). The urea-SCR system with LPV model-based ST-SMC with linear sliding surface is developed.

By applying similar setpoint changes and disturbance in the output, this controller is evaluated and the results are shown in Figures 12 and 13. The settling time and rise in region I are 224 s and 67 s, respectively. The settling time and the rise time for the multimodel PI controller and LPV model-based ST-SMC with linear surface in all regions are also presented in Table 3. The output of the control schemes validated on the urea-SCR system in region I are compared and shown in Figure 14. Even though the proposed controller output is acute compared to the sluggish PI controller output, its practical application will not have any issues as the final control element will be an electronic spray or injection system.

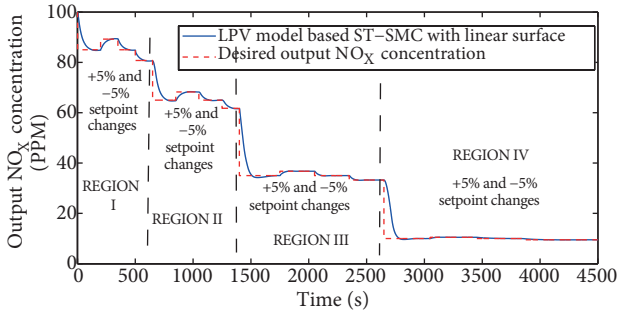

Figure 12. Setpoint tracking of the LPV model-based ST-SMC with linear surface.

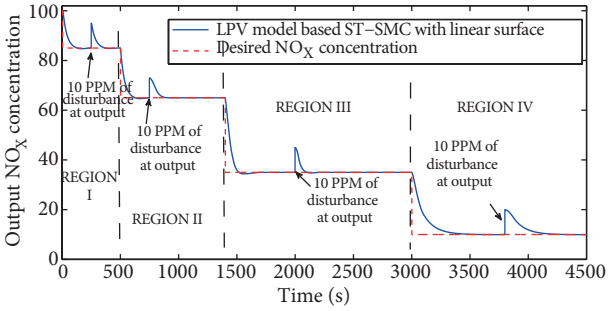

Figure 13. Disturbance rejection of the LPV model-based ST-SMC with linear surface.

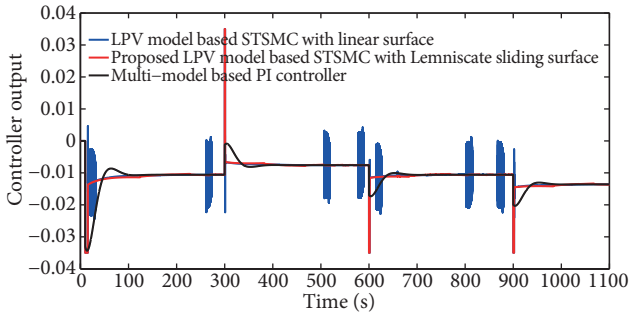

Figure 14. Comparison of the controller outputs in region I for setpoint tracking.

7. Conclusion

A supertwisting sliding mode controller with lemniscate sliding surface is designed to control the NO_X concentration at the outlet of a urea-SCR system. The controller is designed using the LPV model derived from the linear models of the urea-SCR system. The performance of the controller is evaluated by applying step change in the setpoint and disturbance in output and measuring the rise time and settling time for each region. The rise time is found to decrease by 77.32%, 78.91%, 69.95%, and 72.52% in each region and the settling time is found to decrease by 82.35%, 77.74%, 72.33%, and 72.92% in each region as compared to the closed-loop performance obtained with the multimodel PI controller and the ST-SMC with linear sliding surface. The LPV model-based ST-SMC with lemniscate sliding surface algorithm implemented provides faster response and reduces the undesirable chattering effect observed in the conventional SMC. Future work includes experimental evaluation of the proposed control schemes on a urea-SCR system prototype for diesel engines.

References

[1] Koebel DM, Elsener M, Kleemann M. Urea-SCR: a promising technique to reduce NOx emissions from automotive diesel engines. Catal Today 2000; 59: 335-345.

[2] Johnson T. Diesel Emission Control Technology 2003 in Review. SAE Paper 2004-01-0070. Warrendale, PA, USA: SAE International, 2004.

[3] Nova I, Tronconi E. Urea-SCR Technology for deNOx After Treatment of Diesel Exhausts. 1st ed. New York, NY, USA: Springer, 2014.

[4] Upadhyay D, Nieuwstadt MV. Modeling of a urea SCR catalyst with automotive applications. In: ASME International Mechanical Engineering Congress and Exposition; November 2002; New Orleans, LA, USA. pp. 1-7.

[5] Upadhyay D, Nieuwstadt VM. Model based analysis and control design of a urea-SCR deNOx aftertreatment system. J Dyn Syst-T ASME 2006; 128: 737-741.

[6] Devarakonda M, Parker G, Johnson JH, Strots V, Santhanam S. Model-based estimation and control system development in a urea-SCR aftertreatment system. SAE International Journal of Fuels and Lubricants 2008; 1: 646-661.

[7] Devarakonda M, Parker G, Johnson JH, Strots V, Santhanam S. Adequacy of reduced order models for model-based control in a urea-SCR aftertreatment system. In: Proceedings of the SAE World Congress; 2008. Paper 2008-01-0617.

[8] McKinley TL. Adaptive model predictive control of an SCR catalytic converter system for automotive applications. IEEE T Contr Syst T 2012; 20: 1533-1547.

[9] Xu Z, Zhao J, Qian J. Nonlinear MPC using LPV model. Ind Eng Chem Res 2009; 48: 3043-3051.

[10] Vijayalakshmi S, Manamalli D, PalaniKumar G. Closed loop experimental validation of linear parameter varying model with adaptive PI controller for conical tank system. Control Eng Appl Inf 2014; 16: 12-19.

[11] Utkin V. Sliding mode control. Int J Control 1993; 57: 1003-1259.

[12] Bartoszewicz A, Patton RJ. Sliding mode control. Int J Adapt Control 2007; 21: 635-637.

[13] Mizoshiri T, Mori Y. Sliding mode controller with lemniscate sliding surface. In: Proceedings of the SICE Annual Conference; July 2015; Hangzhou, China.

[14] Davila A, Moreno JA, Fridman L. Optimal Lyapunov function selection for reaching time estimation of super twisting algorithm. In: Proceedings of the 48th IEEE Conference on Decision and Control; December 2009; Shanghai, China. New York, NY, USA: IEEE. pp. 8405-8410.

[15] Chalanga A, Kamal S, Fridman L, Bandyopadhyay B, Moreno JA. How to implement super-twisting controller based on sliding mode observer?. In: Proceedings of the 13th IEEE Workshop on Variable Structure Systems; July 2014; Nantes, France. New York, NY, USA: IEEE. pp. 1-6.

[16] O'Dwyer A. Handbook of PI and PID Controller Tuning Rules. 2nd ed. London, UK: Imperial College Press, 2006.